Spatial Patterns of Permafrost at Hoher Sonnblick (Austrian Alps) - Extensive Field-measurements and Modelling Approaches

Wolfgang SCHÖNER[1)*)], Lorenz BOECKLI[5)], Helmut HAUSMANN[1)4)], Jan-Christoph OTTO[3)], Stefan REISENHOFER[1)], Claudia RIEDL[2)] & Sirri SEREN[1)]

[1)] Central Institute for Meteorology and Geodynamics (ZAMG), Vienna, Austria;

[2)] Central Institute for Meteorology and Geodynamics (ZAMG), Salzburg, Austria;

[3)] University Salzburg, Institute of Geology and Geography, Salzburg, Austria;

[4)] Institute of Geodesy and Geophysics, Vienna University of Technology, Vienna, Austria;

[5)] University of Zürich, Institute of Geography, Zürich, Switzerland;

[*)] Corresponding author, wolfgang.schoener@zamg.ac.at

KEYWORDS

ground surface temperature
permafrost monitoring
borehole measurements
mountain permafrost
permafrost mapping
Hoher Sonnblick
geophysics

Abstract

Spatio-temporal patterns of permafrost have been monitored in the Sonnblick region (Austrian Central Alps) since 2006, capturing both permafrost in bedrock at the summit of Sonnblick as well as permafrost in the debris cover of two slopes with different aspect (North and South, with an area of about 1.5km² for each test field). The monitoring covers measurements in boreholes, at the ground surface, by geophysical methods (ground penetrating radar GPR, seismic) and laser scanning, respectively. Additionally, extensive meteorological measurements are available from the Sonnblick Observatory. From these measurements it is evident that detection of significant temporal changes of permafrost patterns clearly need longer observation periods. However, there are first clear results on spatial patterns of permafrost in the Sonnblick region. For the summit area of Sonnblick GPR measurements show a thickness of the debris cover of about 2.5 m, of which the uppermost about 1.5 m are the active layer (derived from borehole temperatures). From borehole tomography a thickness of jointed bedrock with open, probably ice-filled joints, down to a depth of about 9 m was derived. Simulations of ground temperatures of the Hoher Sonnblick summit pyramid with a physical-based model approach indicates that permafrost is restricted to north-facing slopes, whereas south-facing slopes have only sporadic permafrost. Measurements from a spatially dense ground surface temperature network from the two slope sites, however, indicate that permafrost is probable in the Sonnblick region at elevations above 2500 m a.s.l. for north-facing slopes and above 2750 m a.s.l. for south-facing slopes. The data from the slope sites coincide in 60% of the locations with an empirical model approach developed for the Austrian Hohe Tauern region.

Räumliche und zeitliche Muster des Permafrostes werden im Gebiet des Hohen Sonnblicks (Österreichische Zentralalpen) seit 2006 im Rahmen eines Monitorings erfasst. Es wird sowohl der Felspermafrost der Gipfelpyramide des Sonnblicks als auch der Hangpermafrost zweier unterschiedlich exponierter Versuchsfelder untersucht. Das Monitoring beinhaltet Messungen in Bohrlöchern, an der Oberfläche mittels geophysikalischer Methoden und Vermessungen mit einem Laserscanner. Die vorliegenden Ergebnisse zeigen, dass die Messperiode für die Bestimmung von zeitlichen Veränderungen noch zu kurz ist. Jedoch können erste signifikante Aussagen zu den räumlichen Mustern im Sonnblickgebiet gemacht werden. Für den Sonnblickgipfel zeigen die Bodenradarmessungen eine Schicht von ca. 2,5 m von aufgelockerten Fels und Blockwerk, wovon ca. 1,5 m der Auftauschicht zuzuordnen sind (aus den Bohrlochmessungen abgeleitet). Aus der Anwendung einer Bohrlochtomographie lässt sich eine Mächtigkeit des geklüfteten Felskörpers bis ca. 9 m Tiefe ableiten, der vermutlich leicht geöffnete mit Eis gefüllte Spalten aufweist. Die Anwendung eines physikalisch basierten Modelles zur Bestimmung der Temperaturverteilung in der Gipfelpyramide des Sonnblicks legt nahe, dass Permafrost im Wesentlichen auf nördliche Expositionen beschränkt ist, in süd-orientierten Bereichen jedoch nur sporadisch vorkommt. Die Messungen eines dichten Netzwerkes von Oberflächentemperatursensoren in zwei Hangbereichen im Sonnblickgebiet legen nahe, dass Permafrost für Nordexpositionen in Seehöhen über 2500 m und für Südexpositionen in Seehöhen über 2750 m wahrscheinlich ist. Diese Oberflächentemperaturmessungen bestätigen an 60% der Messstandorte eine unabhängige empirische Modellierung der Permafrostverbreitung im Sonnblickgebiet.

1. Introduction

Permafrost (perennially frozen ground) is defined as material of the lithosphere that remains at or below 0°C for at least two consecutive years (e.g. Haeberli and Hohmann, 2008). However, the relationship between changes of the permafrost and climate forcing is complex and dependent on various meteorological and geomorphological conditions. Thus long-term observations covering ground temperatures as well as the surface conditions and the forcings from the atmosphere (such as radiation, air temperature etc.) are needed in order to quantify changes of the permafrost from underlying climate changes. For the European Eastern Alps the monitoring of the permafrost and its changes are hampered not only from the weak signal-to-noise ratio of ground temperature trends but also from the discontinuous structure of the permafrost. Observa-

tions during the last few years showed that subsurface temperatures are significantly affected by heat waves, which in turn result in increased rock fall activity due to the destabilization of ice-filled discontinuities (Gruber, 2005). The Swiss network PERMOS reported a significant increase of the active layer depths in the summer 2003 (Vonder Mühll et al., 2008), maximal changes from 4 m (1999-2002) to 9 m (2003) were observed at the site Schilthorn (2970 m). Wegmann et al. (1998) emphasized that from frost weathering, due to freeze and thaw cycles, considerable amounts of water in joints might also exist in deeper layers of the permafrost bedrock.

Interestingly, systematic permafrost research and monitoring is a rather new research activity in Austria (compared to e.g. Switzerland), though the relevance of know-how on permafrost is obvious for building Alpine infrastructures at high elevations. This statement on research activities is particularly true for bedrock permafrost, whereas systematic studies on rock glaciers started already much earlier in Austria (Lieb, 1991, 1998, Krainer and Mostler, 2000). First measurements of ground temperatures in bedrock in Austria were established at Sonnblick mountain (3105 m a.s.l.), in the Hohe Tauern region (Austrian Central Alps) in 2006. The monitoring was significantly motivated from problems related to possible instability of the buildings (observatory and hut of Alpenverein) at Hoher Sonnblick from permafrost decrease (Schober, 2002) and related construction works for stabilization of the summit pyramid. About the same time an extensive observation network for ground surface temperatures and a snow monitoring (Project PERSON) were installed at two test-fields close to Sonnblick summit (Fig. 1). In the period from 2008 to 2011 Sonnblick was study site within the EU-PermaNet project.

The application of geophysical methods for studying permafrost relies on the physical properties of different earth materials which change with freezing of incorporated water and therefore the formation of varying amounts of ground ice (Scott et al., 1990). Typical geophysical applications for mountain permafrost are mapping, structural exploration and monitoring (Vonder Mühll et al., 2002; Hauck and Vonder Mühll 2003; Hauck et al., 2003; Hausmann et al., 2007; Kneisel et al., 2008). The physical structure of permafrost in bedrock and its temporal changes were successfully investigated by geoelectric and seismic methods (Krautblatter and Hauck 2007; Hilbich et al., 2008; Krautblatter et al., 2010; Draebing and Krautblatter, 2011). Recent studies highlight the high potential of time-lapse seismic tomography to detect temporal changes such as the permafrost degradation (Hilbich, 2010).

This paper summarizes the results of the permafrost monitoring in the Sonnblick region since 2006 from a combination of observational methods and two modelling approaches. All field observations and the modelling approaches are described in chapters 3 and 4. Chapter 5refers to the results of the observations and modelling studies and chapter 6 concludes our results. For Sonnblick summit the study focuses on the documentation of permafrost in bedrock and subsequent debris cover and its reaction to climate change, based on measurements of rock temperature, seismic velocities, and electromagnetic wave velocities. The investigation from two test fields situated in different oriented slopes aims to quantify the relationship between climate forcing and local distribution of permafrost in debris cover from spatially dense measurements of surface ground temperatures and spatial distribution of snow.

2. The study site Hoher Sonnblick

The Hoher Sonnblick is located in the Austrian Central Alps (Fig. 1) and is characterised by the complex geology of the "Tauernfenster" (see Schober, 2002). The summit of Hoher Sonnblick is at an elevation of 3105m a.s.l. and is part of the Alpine main divide, which is a clear climate border between the wetter North (Salzach valley) and the dryer South (Möll valley), clearly reflected in the precipitation patterns and the snow cover distribution close to Sonnblick summit (Auer et al., 2002). Both the northern and southern side of Hoher Sonnblick are covered by small glaciers (ca. 1 km^2) which are subject of detailed glaciological investigations (Schöner et al., 2012). The Sonnblick Observatory at the summit of Hoher Sonnblick is an outstanding research station covering studies and monitoring of the atmosphere, the hydrosphere, the cryos-

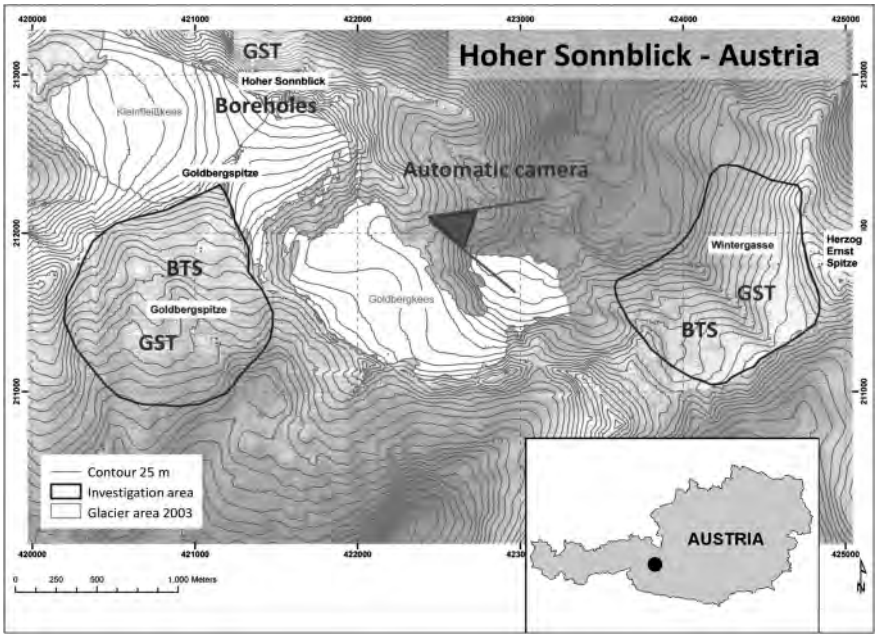

Figure 1: Permafrost monitoring in Hoher Sonnblick region covering bedrock permafrost at Hoher Sonnblick summit as well as permafrost in slopes from two test fields exposed to the North and South, respectevily.

Figure 2: GPR device Spidar in action at the Sonnblick.

phere, the lithosphere and the biosphere (see e.g. Schöner et al., 2012).

Spatial characteristics as well as temporal changes of the climate of Hoher Sonblick and of the larger region of Hoher Sonnblick were described in many studies (see e.g. Auer et al., 2002 and references therein). Thus climate characteristics of the Sonnblick region in particular with relevance for permafrost distribution can be well described from earlier studies. Mean annual air temperature at Sonnblick Observatory is -4.7 C°, annual precipitation is 2500 mm. (mean values for 1971-2000). The air temperature has increased by about 2°C since the beginning of the meteorological observations at Hoher Sonnblick in 1886. Today the mean percentage of solid precipitation on total precipitation during the summer half year (April-September) is about 70% but has significantly decreased since the begin of observations in 1886 by about 15-20% because of increasing temperatures (see Auer et al., 2002). Additionally, the number of frost days (days with minimum temperature below 0°C) and the number of ice days (maximum below 0°C) clearly decreased during this period. Thus it can be concluded that changes of the climate in the last ca. 125 years have been unfavourable for permafrost, not only in the study region but also for the Alps in general. In contrary to permafrost, which is not adequately documented over a longer period, the strong glacier retreat in the Sonnblick region since the maximum extent of the glaciers at the end of the Little Ice Age around 1850, also forced from climate change, is well documented since 1896 (Auer et al., 2002).

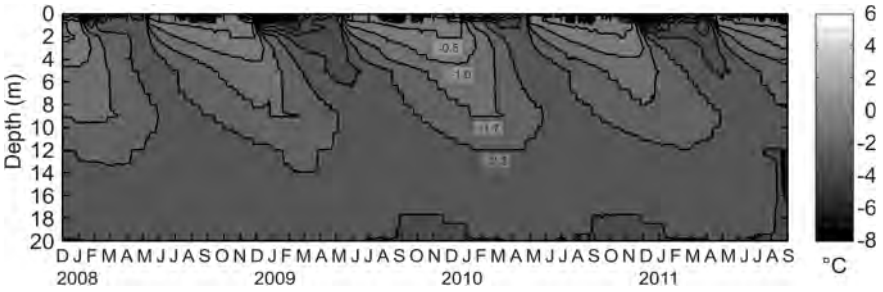

Figure 3: Time series of bedrock temperatures at depths up to 20m measured in the borehole closest to the summit of Hoher Sonnblick for the period December 2007 to September 2011.

3. Measurements

3.1 Borehole measurements

3.1.1 Temperature

On the south-facing slope of Sonnblick summit three 20 m deep boreholes and one 10 m deep borehole were drilled during geotechnical construction works (for stabilisation of the summit) in September 2005. The average slope gradient for the area between the highest and the lowest borehole is 27° and the altitude difference is about 34 m. The highest borehole is located next to the Observatory; the lowest borehole is close to a permanent snow field and the nearby glacier Goldbergkees. The thickness of the debris layer around the boreholes is about 2 m or less. The 20 m deep boreholes were equipped with temperature sensors and geophones, whereas the 10 m deep borehole was equipped with extensometers (project 'Permafrost in Austria') in August 2006. AD592 Precision IC temperature transducers were used and were calibrated before installation by “Sommer Mess-Systemtechnik”. Measuring interval of temperature sensors was 15 minutes which are averaged to hourly means. The estimated accuracy of sensors is 0.1 K.

3.1.2 Seismic tomography

In order to investigate spatial and temporal changes of permafrost in bedrock a seismic borehole tomography was applied. The used seismic layout focused on the registration of inter-annual changes and processes which exist in deeper regions, in addition to the analysis of known processes in the active layer (thawing/freezing). In particular, the layout of the tomography consisted of three strings of geophones installed in boreholes along a south directed profile at the summit of Sonnblick (Fig. 4a). The distance between the boreholes is ~ 30 m. Seismic energy was provided on the surface by a 5 kg hammer (and a plastic plate) at an interval of ~ 3m and were simultaneously registered at 15 borehole geophones. The excitation points were arranged along the main profile and also spatially off-set. The geophones (I/O, SM-4, 8 HZ) were positioned at depths of 1, 2, 5, 10, und 20 m and were connected to single recorders (RefTEK 130, 6 channels). The source signal was recorded by a RefTEK 130 using a sample rate of 1000 Hz and a vertical stacking of 16. The achieved data set includes four campaigns between 2008 and 2009. For each year we documented the times when the active layer was still frozen (July) and when the active layer reached a maximum thickness (~ 0.5 m in September). Measurements repeated at the end of each campaign clearly show that the selected excitations points were stable and that the source signal was reproducible. A 3-D first arrival tomographic inver-

sion of about 1400 P-wave travel times was computed by using the code of Hole (1992). For the inversion a 3-D model with a cell size of 1 m and 3 smoothing iterations was used. As initial model we used a mean 1-D velocity function that was calculated from the up-hole times for each borehole. Initial models with high and low gradients were tested, too and converged to the final model.

3.2 Bottom temperature of snow cover (BTS) and ground surface temperature (GTS) measurements

The monitoring network includes two study sites (Fig. 1, test fields Goldbergspitze and Wintergasse) with measurements of ground-surface temperature (GST) and bottom temperatures of the snow cover (BTS). Whereas test field Goldbergspitze is exposed toward South, Wintergasse is exposed toward North, in order to capture the influence of aspect and related incoming global radiation on ground surface temperatures and permafrost distribution. GST have been measured with UTL1 and UT2 loggers (for number and location see Figures 12 and 13), BTS measurements have been carried out by BTS probes each winter in February to March since 2006, depending on weather conditions and avalanche danger. In addition to the test-fields Goldbergspitze and Wintergasse 35 temperature logger (20 UTL-1 and 2 datalogger and 15 tidbits) were installed in the summit area of Hoher Sonnblick in autumn 2006 for measuring surface rock temperatures during the entire season. 20 logger of the types UTL-1 and 2 were installed on moderate slopes on the southern side of the summit. In the steep north face 15 tidbits were installed.

In order to measure the ground temperatures more precisely, in particular to reduce the atmospheric influence on the sensors, five boreholes with depths between 30 cm and 140 cm were drilled in the study site Wintergasse using a petrol powered drill in autumn 2010. Two boreholes were equipped with 4 temperature sensors at intervals of 20 cm, one borehole with two temperature-sensors at a vertical distance of 40 cm. Each temperature logger was barred by insulating foam above and below the sensors. The insulation has a twofold role: thermal barrier between the sensors as well as barrier between various atmospheric influences and the temperature sensors.

Quantifying the influence of the spatial and temporal development of the winter snow cover on permafrost distribution is another task of the monitoring. This has been achieved by an automatic monitoring camera which was installed on the opposite slope of the study area Wintergasse in the year 2008. The camera – Type Nikon D80 with a 24-mm lens and an interval timer– took three pictures per day in order to raise the probability of one useful photograph per day (considering the high number of foggy or cloudy days).

3.3 GPR measurements

Ground Penetrating Radar (GPR) measurements were carried out in September 2009 and November 2010, respectively. The GPR device “PulseEkko PRO” with a 500 MHz Antenna and odometer wheel was used for the 2009 campaign. However, stone plates on the surface did not allow a good coup-

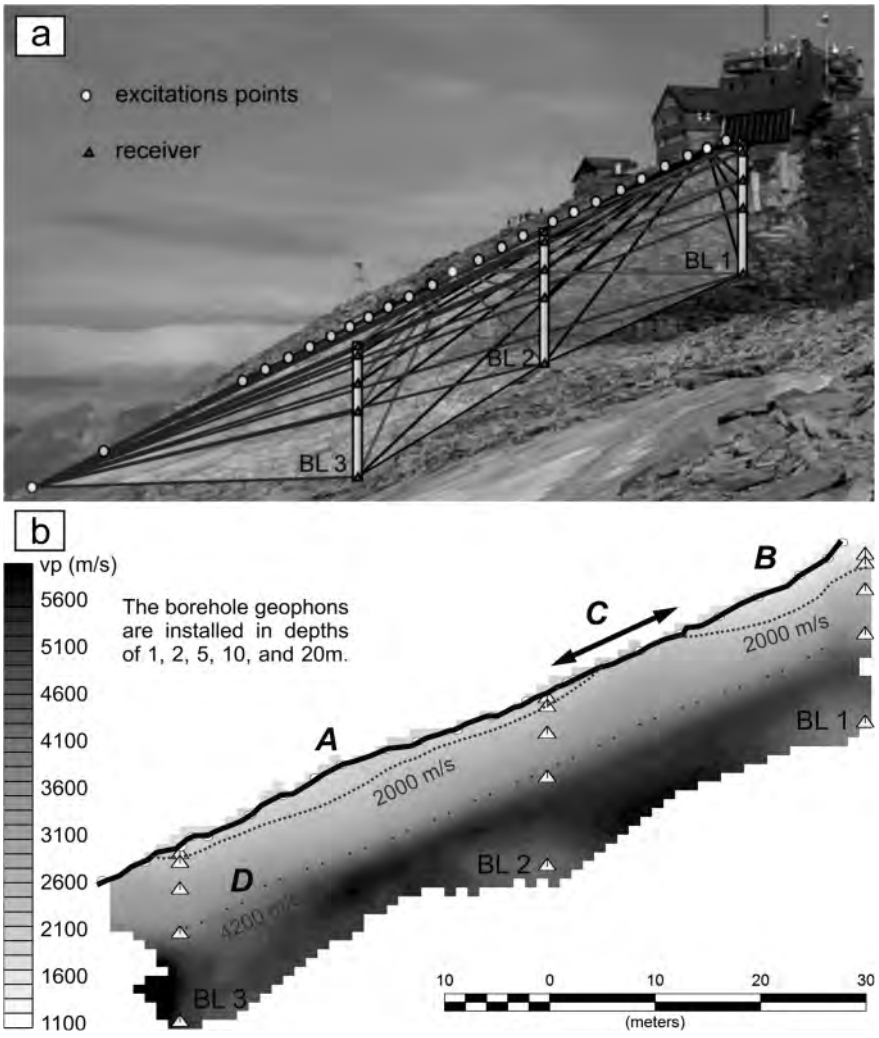

Figure 4: Layout and P-wave velocity model of the seismic tomography at the summit of Hoher Sonnblick. The boreholes are denoted as BL1-3. (a) Sketch of the tomography with ray coverage (at 3 stations), source and receiver geometry. (b) 2-D velocity model along the main profile with interpretations (A-D). Strong lateral variations are displayed in near-surface regions: Low velocities are imaged under a ridge (A) or near to the summit (B) and high velocities are imaged in a region with long-lasting snow cover (C). For deeper regions a strong gradient is recorded at depths of 8 - 10 m (D).

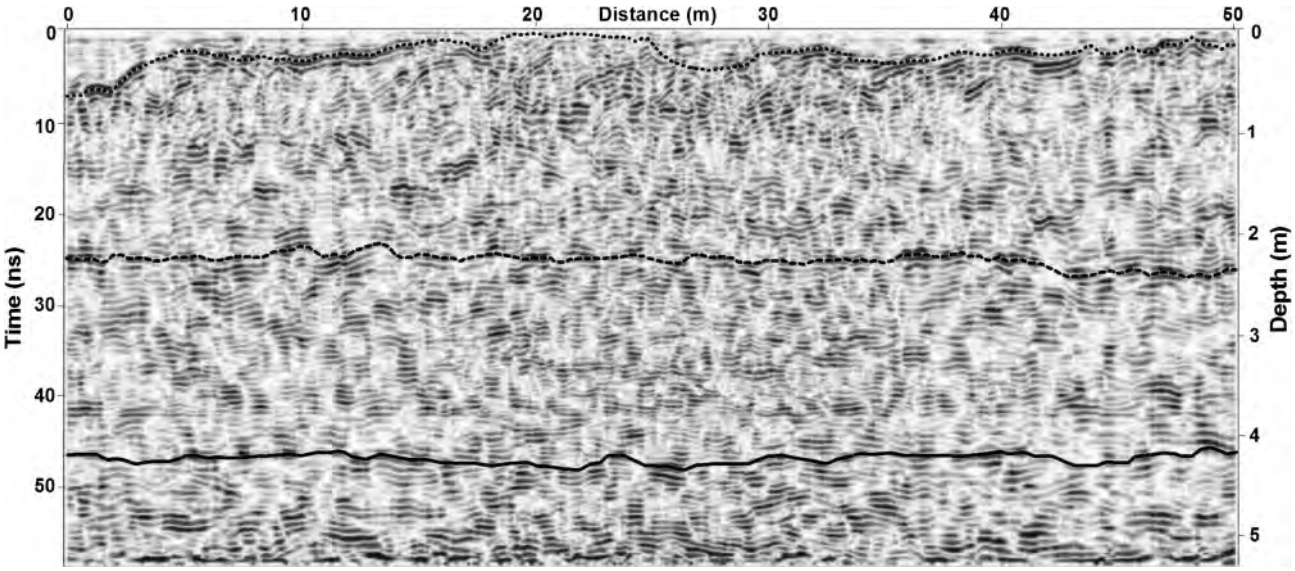

Figure 5: GPR profile from the summit region of Hoher Sonnblick measured in September 2009 recorded by using a Pulse Ekko PRO.

ling between antenna and the ground, and the distance measurement by the odometer wheel was inaccurate.

For the second GPR measurement in November 2010 the GPR device "SPIDAR" with 5-channels equipped with 500 MHz antennas was adapted (Fig. 2). This time the contact between the antennas and the ground was good, as the survey area (35 x 58 m) was completely covered by snow. The survey grid was 5 x 50 cm, with a total of 70 measured lines using the SPIDAR device. Positioning of the lines was done by differential GPS (DGPS).

3.4 Terrestrial 3D laser scanning

Data were recorded with the 3D laser scanner "RIEGL LMS-Z420i" which was combined with a calibrated digital camera "NIKON D100". The first measurement campaign was in September 2008, the second one in September 2010. For both field campaigns identical 8-scanning positions were used. The mean error of distance measurements was approximately 1 cm and spatial scanning was done every 5 cm.

4. Model approaches

4.1 Regional permafrost distribution from empirical Permalp/Permakart method

We used an adapted and modified version of the permafrost model Permakart developed by Keller (1992) to model regional permafrost distribution. Permakart is an empirical-statistical model that uses the observed relationship between topography and climate influencing the occurrence of Alpine permafrost. These observations have been formulated as rules-of thumb by Haeberli (1975) and represent a topo-climatic key of permafrost occurrence based on the topographic parameters slope, aspect and elevation. By analysing the topographic parameters elevation is used as a proxy for temperature change and aspect serves to represent solar radiation effects. Furthermore, different slope classes are applied representing the influence of the snow cover on the permafrost distribution. The topo-climatic key contains 48 classes of permafrost limits for different aspects and 3 different slope angle classes (foot slopes, steep slopes, bedrock slopes). Originally, the Permakart model contained two permafrost classes, "permafrost possible" and "permafrost probable", in accordance with the BTS classification (Haeberli, 1973, Piemonte, 2011). In the actual version of Permakart, this classification was transferred to an index of occurrence between 1 and 100. The index represents an analogy to a probability of permafrost occurrence without being a real statistical probability. An index value of 50 indicates the boundary between the original classes of "permafrost possible" and "permafrost probable". The actual

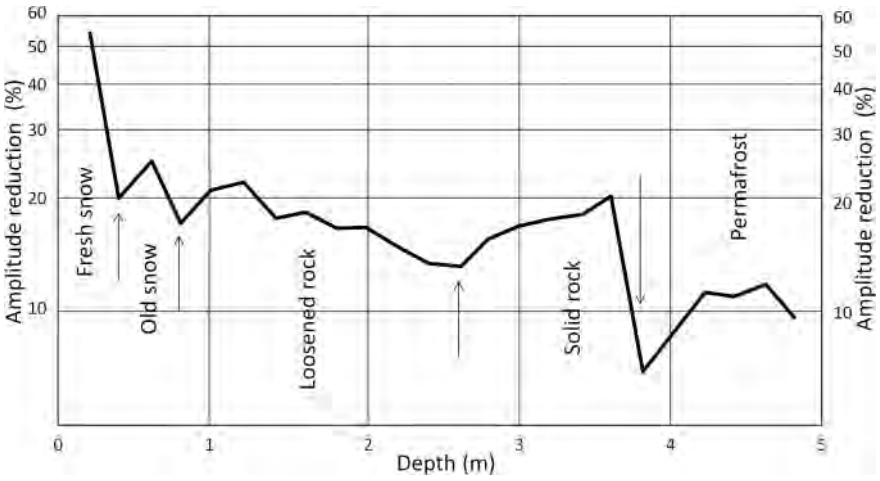

Figure 6: Amplitude reduction of the GPR data from September 2010 with APRADAR software.

version of Permakart were adapted to the observed permafrost conditions in the Hohe Tauern range based on the previously published permafrost limits of Lieb (1998) and recent field data (BTS, GST, ERT, GPR). Permafrost modelling was performed using a 10 x 10 m digital elevation model (DEM) provided by the province of Salzburg (SAGIS). Foot slopes were derived using a resampled 50 x 50 m resolution DEM. The presented map of permafrost distribution in the region of Hoher Sonnblick is a blow-up of the new permafrost map of the Hohe Tauern, compiled within the Permalp.at project. More details on the Permakart model applied for the Hohe Tauern region and the map of permafrost distribution can be found at the website www.permalp.at.

4.2 Physical-based modelling of ground temperatures of Sonnblick summit pyramid

The modelling of ground temperatures was done by the Department of Geography, University of Zurich in the frame of the Alpine-Space Program PermaNET and was based on two major steps: a) Simulation of the spatial patterns of near-surface temperatures using the energy-balance model GEOtop (www.geotop.org). b) Three dimensional modelling of ground temperatures based on heat conduction with COMSOL Multiphysics (COMSOL AB, Stockholm). For this purpose the near-surface temperatures were used as upper boundary conditions. Simulations were based on the approach shown by Noetzli (2008), which were tested and applied for modelling the 3D temperature distribution in steep alpine terrain. (e.g., Noetzli, 2008; Noetzli and Gruber, 2009).

GEOtop (Bertoldi et al. 2006, Rigon et al. 2006, Endrizzi 2009, Dall'Amico et al. 2010) simulates spatially distributed near surface temperatures in complex terrain forced by climate data and ground characteristics. The model couples the energy and water balance, including phase changes in the ground. The snow module of GEOtop allows simulating a multi-layer snow cover. As ground temperatures in mountains are significantly influenced by the snow cover and related redistribution processes, a simple algorithm that reduces the snow cover in steep terrain is implemented. Depending on the slope angle, a correction term is multiplied with precipitation for each grid cell. Additionally, snow-transport by wind is parameterized according to Pomeroy et al. (1993).

The subsurface temperatures were calculated by GEOtop based on a finite element mesh (fe mesh) with increasing mesh size towards the surface. In addition the conductive heat transfer, the effect of latent heat during phase change from ice to water is considered (Noetzli and Gruber, 2009) by the model. Temperatures in deeper layers are strongly influenced by past cold climate conditions (Haeberli et al., 1984) and actual subsurface temperatures are colder than for a stationary temperature field that corresponds to current climate conditions (Noetzli and Gruber, 2009). Therefore, past climate changes need to be considered to estimate current ground temperatures. Consequently, the upper boundary condition (surface temperatures) was changed with time and thus transient simulations were possible. In particular, we assumed that changes in surface temperatures follow measured air temperatures and are uniform within the whole modelling domain.

Input parameters and boundary conditions:

A digital elevation model (DEM) with a grid spacing of 10 m was used for the GEOtop simulations. The fe mesh that was required for the simulations with COMSOL and consisted of 69,246 elements in total. The model domain included the entire summit of Hoher Sonnblick and large parts of its north face. The forcing of GEOtop was based on climate data from the station at Hoher Sonnblick and covered the parameters air temperatures, wind speed, wind direction, relative humidity, global radiation and precipitation. The used time series started at July 1986 and ended in May 2011.

The aim for the simulations with GEOtop was to estimate the spatial patterns of surface temperatures and related uncertainties. We used the following strategy to capture a larger scatter of surface temperatures caused by climatic forcing: 12 different two years sub-periods were simulated using climate data for the years 1986–1988, 1988–1990, up to 2008–2010, res-

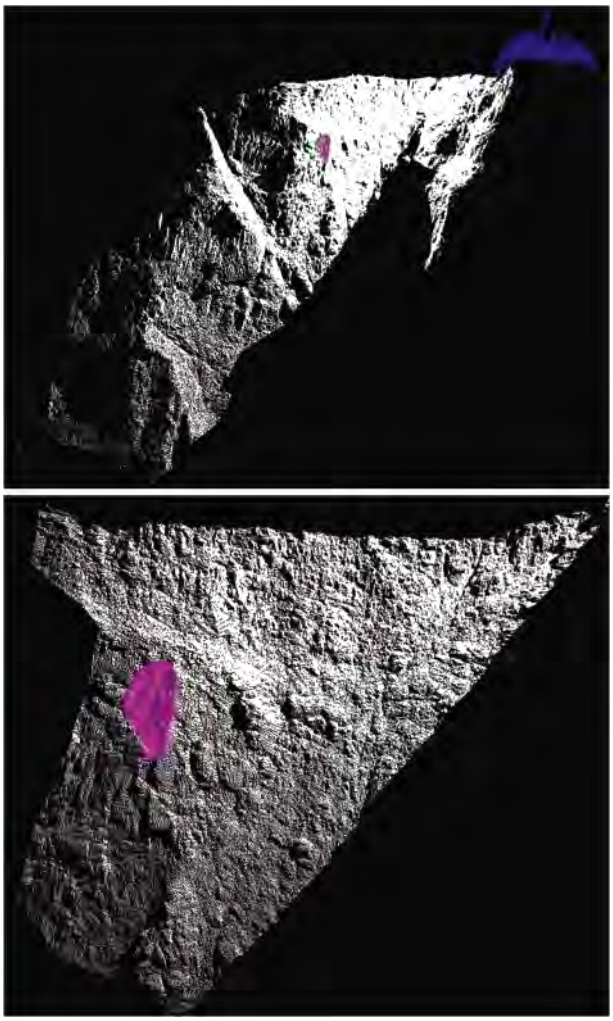

Figure 7: Laserscan of summit of Hoher Sonnblick with Sonnblick Observatory marked in blue, left: complete north wall, right: blow-up showing the region with biggest mass movement derived from the scans in 2008 and 2010 (pink area).

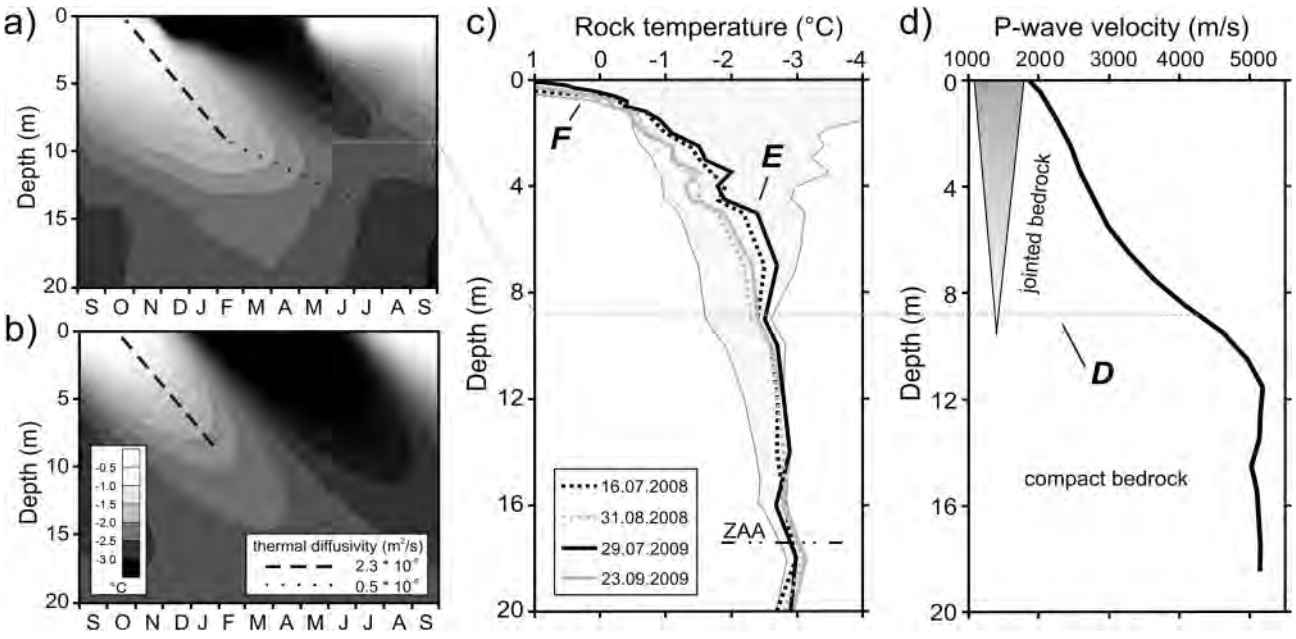

Figure 8: The observed (a) and modelled (b) annual temperature wave and the comparison of rock temperature (c) and seismic P-wave velocity (d) along with depth. For the rock temperatures the zero annual amplitude (ZAA) and the envelope of amplitudes recorded in 2008 and 2009 (grey area) are displayed. The symbol (D) denotes the delineation of jointed bedrock to compact bedrock and correlates with the change of thermal diffusivity in a). In the summer, short term variations extended to a depth of about 9 m (E), whereas the active layer thickness is < 1m (F).

pectively. Besides the variability in surface temperatures caused by climate forcing, snow cover duration and timing were assumed to be other important sources of uncertainties. Therefore it was crucial to evaluate the parameterization of the snow transport algorithm by varying the topographic parameters of the empirical approach. Additionally, the quality of the measured precipitation data is unknown and an error of 10% or more is likely. To address this uncertainty, two correction factors (0.8, 1.2) for the precipitation data were applied in order to reduce or enlarge the precipitation measurements. In total, 48 simulations were calculated with GEOtop. The resulting mean, minimum and maximum of the surface temperatures for each grid cell were used afterwards for the 3 dimensional modelling within COMSOL.

The upper boundary conditions for the three-dimensional modelling were chosen as described above (mean, minimum and maximum surface temperatures). The lateral boundaries are thermal isolated, and the lower boundary heat flux is 0.08 Wm-2 at sea level. For the glaciated area located at the southern part of the summit we assumed a constant surface temperature of 0°C. Glacier retreat in the past was not considered and sub-glacier temperatures were assumed to be constantly 0°C for the initialization. The ground was assumed to be homogenous for the entire summit. The simulations started in the year 1850 with an assumed temperature-reduction of 1.5°C in relation to current conditions. From 1850 onwards the temperature was linearly increased.

5. Results

5.1 Permafrost at the summit

5.1.1 Bedrock temperatures from observations

In Figure 3 the time series of temperature of the borehole

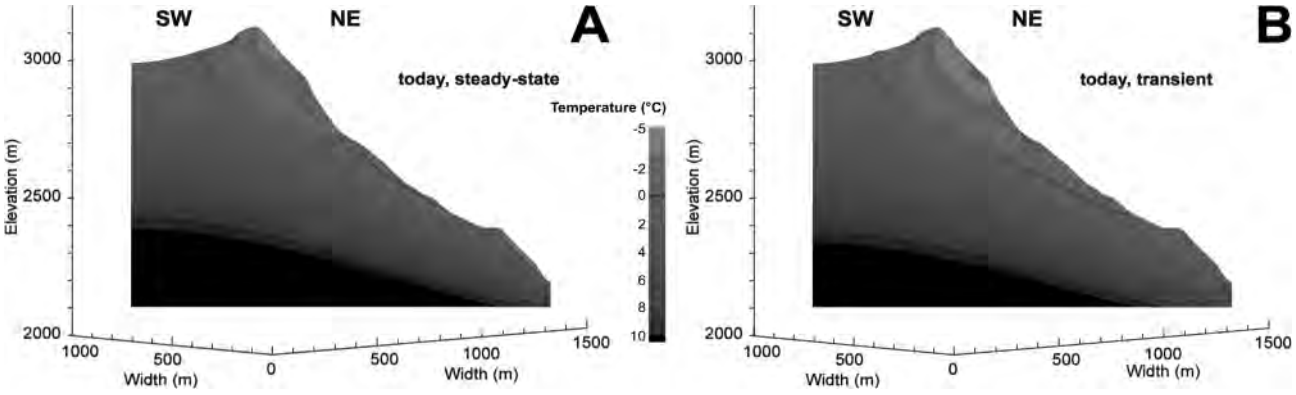

Figure 9: Results of the simulations for the cross sections of the Hoher Sonnblick summit crest: A) today and steady state conditions, B) today and transient conditions. The black line marks the 0° isotherme.

closest to the summit of Hoher Sonnblick is shown for the period December 2007 to September 2011. Due to the very thin snow cover the cold wave could penetrate into the ground more effective in the winters 2008/2009 and 2010/2011 than in the winters 2007/2008 and 2009/2010. The wave of coldest temperatures at the surface arrived with a delay of about four months at a ground depth of 5 m. Temperature measurements indicate that during summer the active layer thickness is about up to one meter at the summit of Hoher Sonnblick.

5.1.2 Seismic tomography

Analyses of seismograms, travel time plots and the computed P-wave velocity field were used to characterize both, the structure and temporal variations of the permafrost. The display of the wave field as offset bin plot (Hausmann et al., 2007; not shown) clearly reveals P- and strong, vertical polarized S-waves for all four data sets. As observed by Hilbich (2010) the September data exhibit a higher spatial coherency due to the complete melting of the seasonal ice in the active layer. The onsets of the P- and S-waves noticeably show a delay for the two September data sets. This is also found in the ordinary travel time plots. Linear regression of the travel time difference plots (not shown) results in mean delays of 2.0 ms (2008) and 1.6 ms (2009) for the P-wave arrivals. Since these delays occur at small offsets we relate them to freezing and thawing processes in the active layer (< 1 m). Additional delays in the travel time differences at larger offsets were not observed (correlation coefficients < 0.17). This indicates that within the investigated two years temporal changes of the rock temperatures in deeper regions of the permafrost did not measurably affect the physical structure of the summit.

The 3-D first arrival tomography reduced the initial RMS error of the travel time residuals from ±4.1 to ±1.9 ms (similar values as in Hilbich, 2010; Draebing and Krautblatter, 2011) and provided a P-wave velocity model for July. The slice through the 3-D tomography (along the boreholes) shows strong lateral variations near the surface (Figure 4b A-D). Extreme low velocities (< 2000 m/s) are imaged below a ridge (A) and near the crest (B). Near-surface velocities were clearly higher within a region of significant longer snow cover duration. At greater depth (8 - 10 m) vertical changes in the velocity field were characterized by a strong gradient (D). Due to the poor ray coverage at depths below 15 m the anomalies near BL1 and BL2 were not interpreted. Velocities between 1500 and 2000 m/s were found to occur in frozen debris with intercalated ice (Hauck and Kneisel, 2008) at depths of up to 2 m. For depths between 2 - 8 m, velocities of up to ~ 3600 m/s were derived which indicates jointed bedrock. Below this depth compact bedrock was detected.

5.1.3 GPR results

The following major processing steps were applied for interpretation of the GPR data:

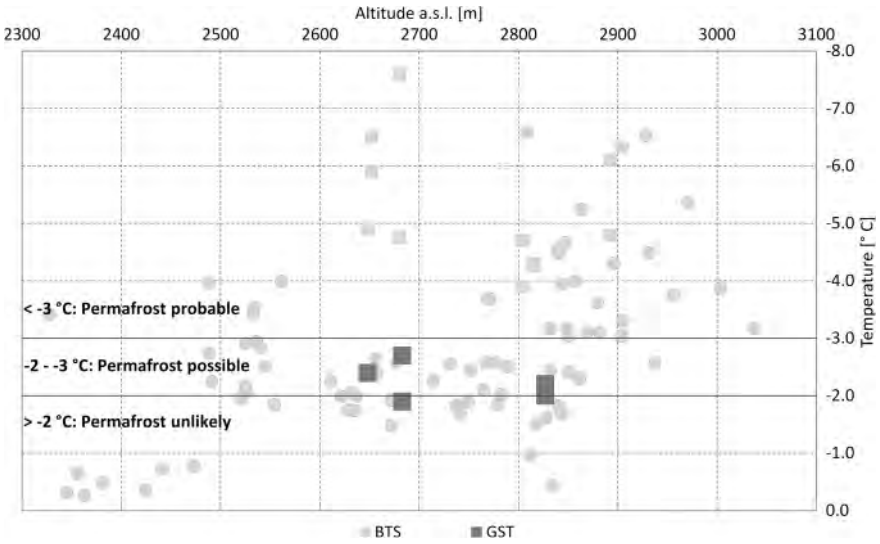

Figure 10: BTS and GST measurements at the study site Goldberspitze – typical threshold values of winter equilibrium temperature (WEqT) were used as indicators. For GST the mean February temperature was used. Light grey squares indicate GST measurements without sufficient snow cover.

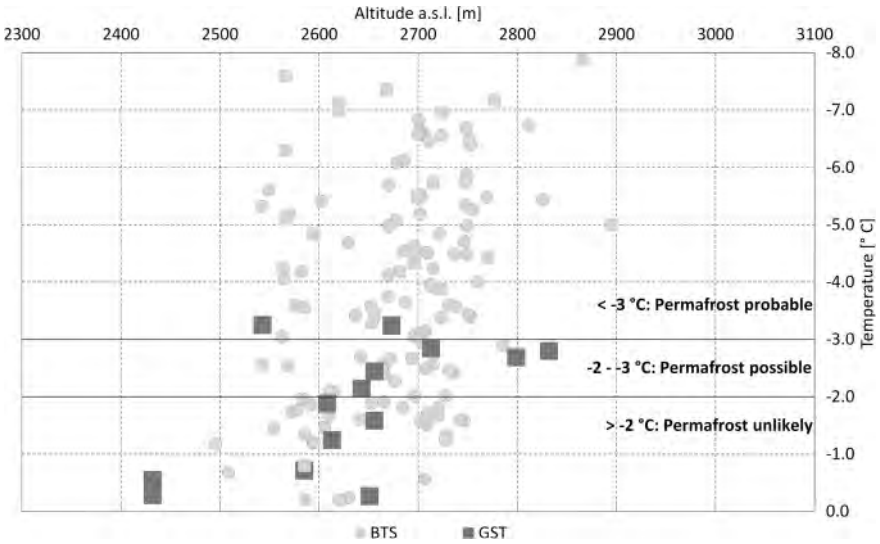

Figure 11: BTS and GST measurements at the study site Wintergasse – typical threshold values of WEqT were used as indicators. For GST mean February temperature was used. Light grey squares indicate GST measurements without sufficient snow cover.

- Editing of the geometry
- Start time correction
- Moving DC-shift
- Dewow filtering
- Dynamic correction
- Bandpass filtering
- Kirchhoff migration and depth conversion

After processing the GPR profile from September 2009 it was interpreted as shown in Figure 5, using a routine which analysis the energy of the EM-waves and thus identifies layers from the reflected energy (APSOFT software). From the interpretation of the shape of reflection-hyperbola in various depths a velocity of 0.18 m/ns was derived and used to compute layer depths from GPR travel times. Three layers were identified. Layer 1 (uppermost layer) correlates with snow. At the beginning of the profile (left side of Fig. 5) an 80 cm thick snow cover was detected, which thins out over a distance of about 20 m. Layer 2 was interpreted as debris cover. The next reflector at a depth of 2.4 m was interpreted as the surface of bedrock, the reflector at a depth of about 4 m as the surface of the permafrost body (which is in fairly good agreement with borehole temperature observations shown in Fig. 3). In the permafrost layer the amplitude of the GPR waves were higher than in the unfrozen rock.

The GPR data from November 2010 were further processed with ZAMG-software “APRADAR” (see Neubauer et al., 2002), which provides the interpretation of the amplitude absorption with increasing depth. Thus layer properties and reflection boundaries could be derived. Figure 6 shows the amplitude reduction with depth for the 2010 data. Four boundaries and five layers can be identified from the figure. The reflection boundaries are indicated at depths of 0.4 m, 0.8 m, 2.6 m and 3.8 m. The successive layers are fresh snow, old snow, debris, bedrock and the permafrost body. The amplitude reduction amounts to about 20%, in snow, debris and bedrock whereas in the permafrost body the reduction is approximately 10%.

5.1.4 Terrestrial 3D laser scanning

The 3D laser scanning data were processed with the software RISCAN PRO. After correction of the scanning data and matching with the digital photographs, all different scanning positions were rejoined to a 3D point cloud. In the next step

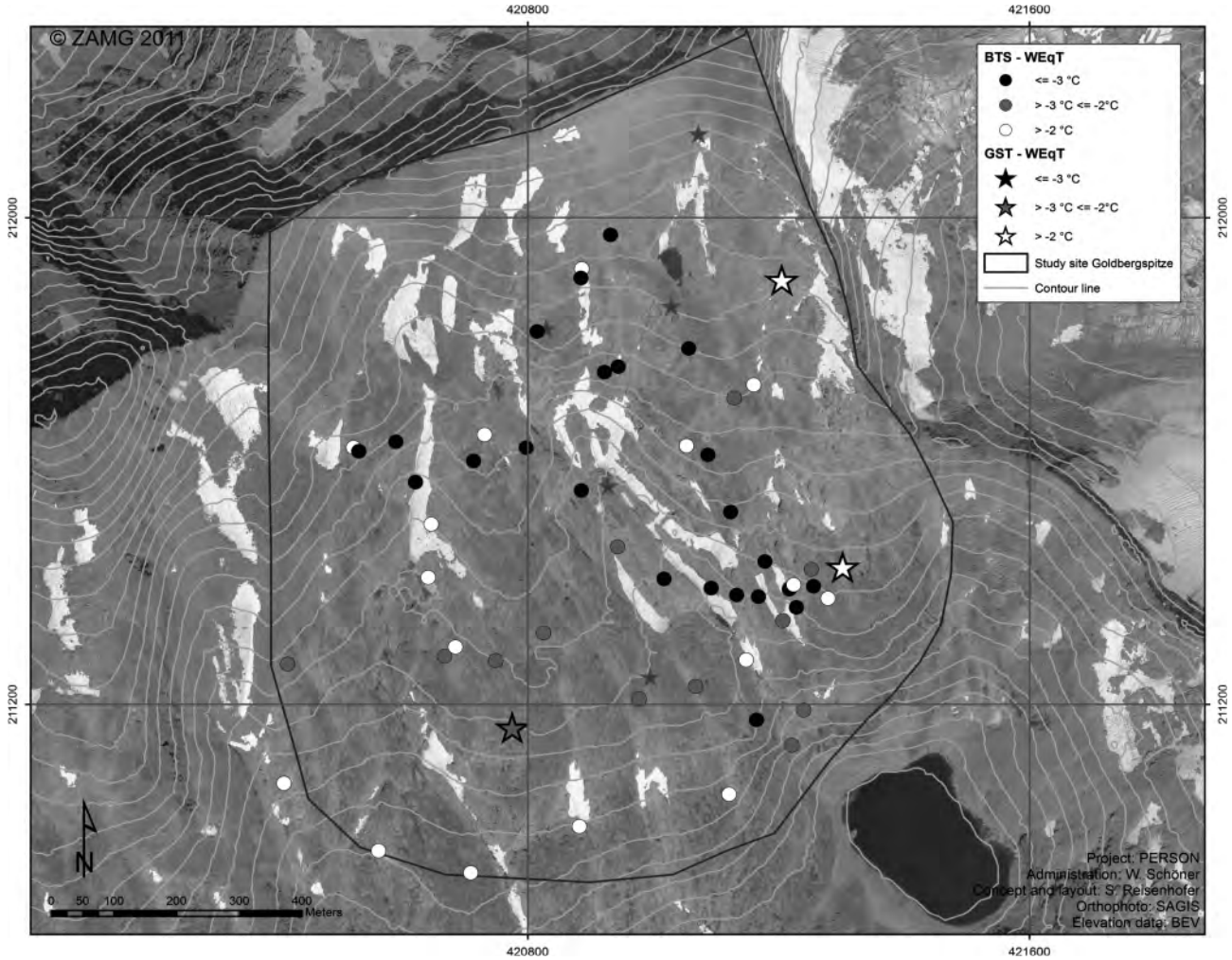

Figure 12: BTS and GST measurements at the study site Goldberspitze – typical threshold values of WEqT were used as indicators. For GST the mean February temperature was used. Light grey stars indicate GST measurements without sufficient snow cover (black stars mean logger sites with missing data).

these data were subjected to triangulation and texturizing. The result was a 3D mesh model of the study region.

Thus it was possible to compare the scanning results from 2008 with those from 2010, because identical parameter and scanning positions were used (Fig. 7).

Due to the size of mass movements, a point grid with 25 cm was computed (scanned points exhibit 1 cm accuracy). The difference of the scanning from 2008 and 2010 was calculated and the surface from 2010 was used as the reference.

Neutral areas (insignificant changes) were plotted in black and white, whereas the cyan coloured areas distinguish the largest mass change. A blow-up of the area with largest mass changes is shown in Figure 7 (right graph). This mass loss area has a length of about 17.0±0.2 m, the calculated volume of the lost block amount to 96±5 m3. This result underlines the active rock fall activity in the region of Hoher Sonnblick.

5.1.5 Synopsis of thermal and seismic structures of the summit

As the seismic tomography indicated jointed bedrock down to greater depths, the thermal properties need to be further investigated. We compiled the observed rock temperatures recorded at borehole 1 for a period of one year and applied a 1-D model for heat conduction (Pogliotti et al., 2008) to describe the annual temperature wave (Hausmann et al., 2010). As parameterization we used a single layer with constant thermal diffusivity. The model fits the observed values for depths between 2 and 8 m and suggests a thermal diffusivity of 2.3E-6 m^2/s. Below this region significant lower values (~ 0.5E-6 m^2/s) and the introduction of an additional layer is required (Figs. 8a,b). Figure 8a shows the temporal changes of the temperature recorded at borehole 1 for the times of the four seismic campaigns.

The derived values for the thermal diffusivity in (E) are of similar order of magnitude as reported from permafrost in rock walls in the Swiss Alps (Wegmann 1998; Pogliotti et al., 2008). In order to compare the temporal variations of the thermal regime with vertical changes in the physical structure we generated a plot of the mean 1-D velocity depth function of the seismic velocities (Figs. 8d). The results of the tomographic inversion indicate jointed bedrock in region (E) which is delineated by (D) from the compact bedrock. Thus the thermal

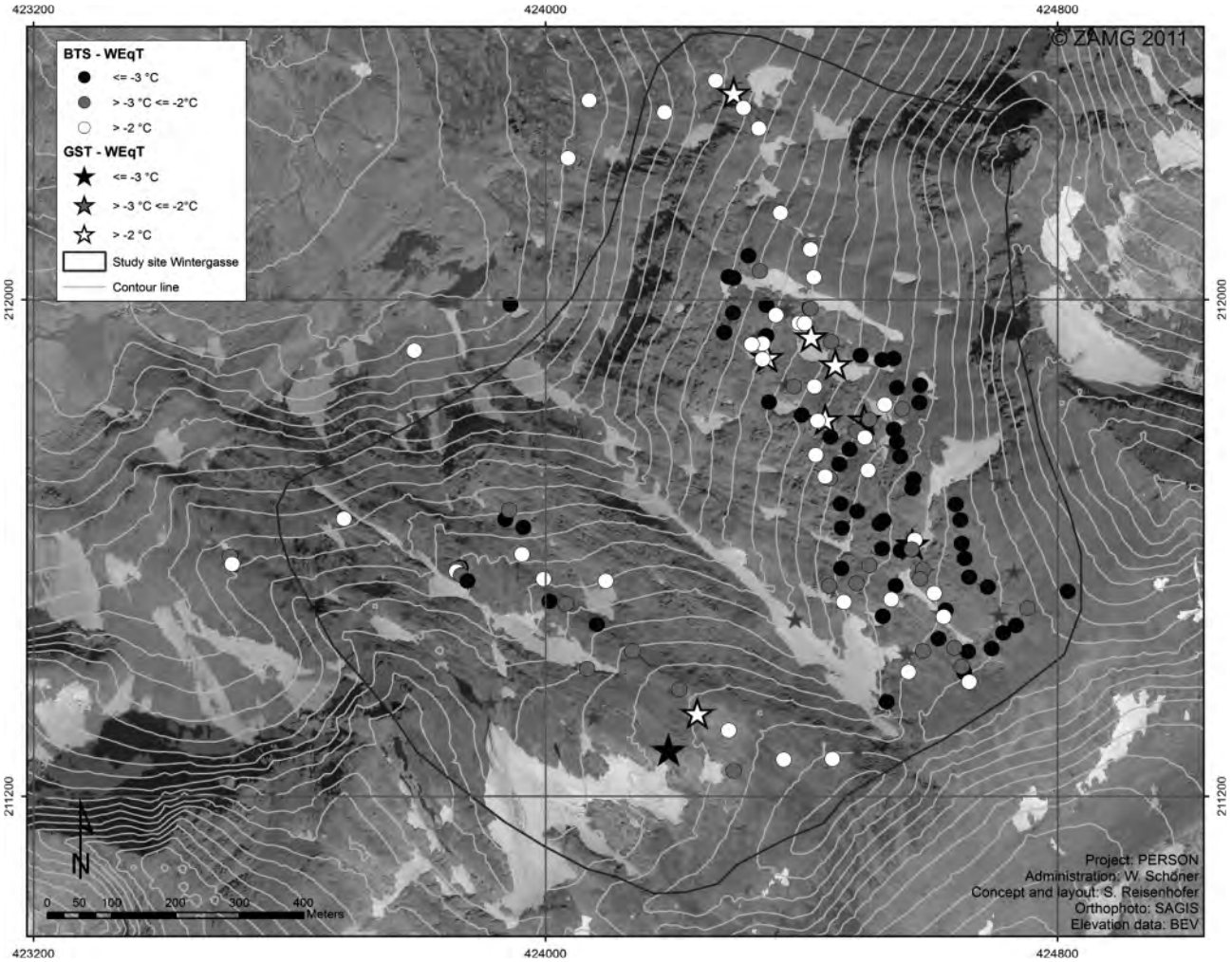

Figure 13: BTS and GST measurements at the study site Wintergasse – typical threshold values of WEqT were used as indicators. For GST the mean February temperature was used. Light grey stars indicate GST measurements without sufficient snow cover (black stars mean logger sites with missing data).

and physical structure at depths of up to ~ 8 m is characterized by a strong heat transfer which corresponds to the zone of jointed bedrock. Below this depth the heat transfer decreases and compact bedrock is found. We explain the temperature changes either from a) air-filled voids enabling very efficient heat transfer within the fissures of jointed bedrock or b) a 3d effect caused by local topography.

5.1.6 Ground temperature distribution from modelling

According to our simulations permafrost exists beneath the crest and on the north facing slopes, whereas in south facing slopes permafrost is sporadic. The lowest modelled temperatures were about -3.5 °C and are simulated for the upper parts

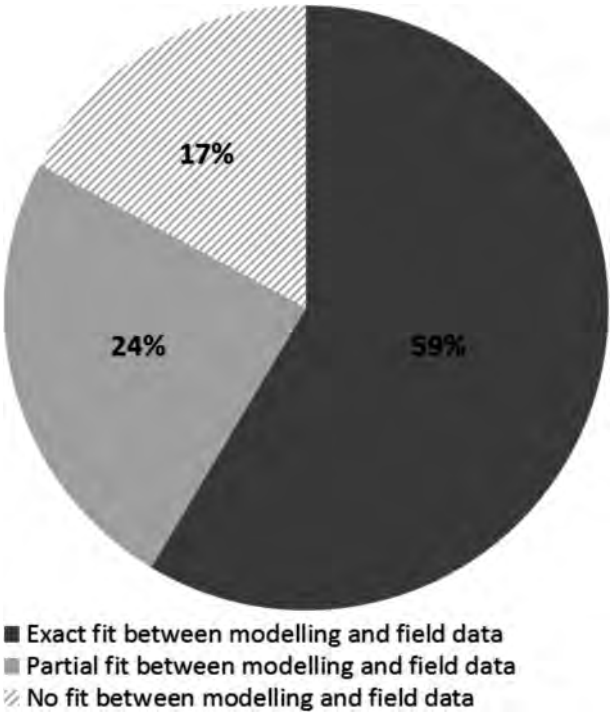

Figure 14: Comparison of field data and modelled permafrost occurrence (Total number of BTS-measurements used: N = 70).

of the north-face of Hoher Sonnblick. The steep terrain as well as the constructions at the summit cause a large heterogeneity of the snow depths and thus permafrost is sporadic in the south facing slopes. Comparison of ground temperature series from a synthetic borehole simulated by the model with observations from the borehole described in Figure 3 shows similar range and patterns.

3D fields of current and future ground temperatures (Fig. 9) have to be interpreted with care, in particular for the southern part of the summit, because glacier retreat was not considered in our model experiment. Interestingly, transient model runs simulate a larger permafrost body in the subsurface than expected from current climate conditions. However, these model results have to be seen in the light of significant uncertainties coming from unknown surface and subsurface conditions (e.g. ice content).

5.2 Regional patterns of permafrost in the Sonnblick region

5.2.1 Spatial permafrost distribution from observations of GST and BTS

All GST and BTS measurements between 2006 and 2011 were compiled together in order to derive spatial patterns of permafrost for the larger region of Hoher Sonnblick. GST observations were checked for atmospheric influence and BTS measurements were checked for exceeding a threshold value of minimum snow depth during the measurements. The results are shown in Figures 10 and 12 for the site Goldbergspitze and in Figures 11 and 13 for the site Wintergasse. In general the spatial variation of ground surface temperatures during winter is rather high, in particular for the southerly exposed site Goldbergspitze. We computed winter equilibrium temperature WEqT for all GST sensors Giving GST a higher weight compared to BTS data we derived as a general rule, that permafrost probably occurs from 2500 m a.s.l. upwards for site Wintergasse and from 2750 m a.s.l. upwards for site Goldbergspitze.

5.2.2 Spatial permafrost distribution from empirical modelling

The Hoher Sonnblick (3106 m) is located at the main divide of the Eastern Alps. The crest and peaks of the divide in this area reach elevations between 2694 (Riffelhöhe) and 3254 m a.s.l. (Hocharn). Two glaciers, the Goldbergkees and the Kleinfleißkees, and numerous small snow and ice fields can be observed around the summit of Hoher Sonnblick. The permafrost modelling classifies more than 50% of the study area around the summit (generally above 2000 m a.s.l., Figure 14) as being affected by permafrost (Table 1). This represents an area of approximately 8 km², compared to less than 3 km² (< 20%) that is covered by glaciers. The permafrost model depicts strong altitudinal and very distinct aspect differences. Permafrost occurrence starts at around 2300 m a.s.l. on north facing slopes, with few isolated zones below. On south facing slopes isolated areas affected by permafrost are modelled above 2500, more continuous zones are observed only above 2900 m a.s.l. Comparing the BTS data shown in chapter 4.2.1 with the modelling results reveals that about 60% of the data show an exact fit between BTS-classification (permafrost possible, permafrost probable, no Permafrost) and permafrost index (Fig. 15). At about 25% of the BTS measurements a partial fit between field data and model is observed. Partial fit means that permafrost was observed and modelled, however the BTS value and the index value did not fall into the same class (for example, BTS data < -3°C and PF index < 50. At 17% of the recorded BTS values, field data and modelling results do not fit at all. This comparison reveals that the adapted Permakart model produces a realistic image of the permafrost distribution around the summit of Hoher Sonnblick. How-

ever, it needs to be regarded that this comparison is between point values and raster cell values of a 10x10 m size. Therefore, local variations smaller than the model resolution may have been detected by the field measurements, but cannot be represented by the model. It is recommended to verify the permafrost distribution around the Hoher Sonnblick with alternative methods including geophysical measurements.

Permafrost	Area (km²)	%
<50%	4,1	29,0
>50%	3,7	26,0
Total	7,8	55,0
Glacier	2,8	18,1
Total Area	23,3	100,0

Table 1: Distribution of Permafrost and Glaciers in the Hoher Sonnblick area.

6. Conclusions

From an extensive monitoring of permafrost in the Hoher Sonnblick region based on a great variety of methods since 2006, we draw the following conclusions for permafrost distribution in the Sonnblick region:

Temperature measurements in boreholes at Hoher Sonnblick clearly show the high influence of surface energy balance on related ground temperatures. Snow accumulation is known to be highly variable at the summit of Hoher Sonnblick, because of the high influence of the summit topography and the buildings on the local wind field and related snow deposition. Consequently, local snow patterns play a crucial role for the temporal evolution of borehole temperatures. The active layer at the summit of Hoher Sonnblick is about 1m thick, derived from borehole temperatures. Borehole temperatures confirm fairly well the estimated permafrost layer interpreted from the data of two GPR campaigns. Interpretation of GPR measurements indicate that jointed bedrock at the summit of Hoher Sonnblick is covered by an approximately 2.5 m thick debris layer.

Seismic borehole tomography was applied for the first time in the Alps in order to investigate spatial and temporal changes of permafrost in bedrock. The combined analysis of the results from the seismic tomography and the rock temperatures reveal new insights on the thermal and physical structure of the summit. Both methods suggest the existence of processes in deeper regions (up to 10 m) which should be monitored further to better understand the future permafrost evolution.

Physical-based modelling of ground temperatures indicates for the summit of Hoher Sonnblick that permafrost is restricted to north and north-east oriented slopes, whereas in south facing slopes permafrost occurs sporadic.

Evaluation of the so far collected data from GST and BTS measurements indicates a major impact from heterogeneous geomorphology and local climate conditions. The results from GST and BTS measurements imply that permafrost occurrence above 2500 m on north–facing slopes and above 2750 m on south-facing slopes are probably. The study period is clearly too short to give a significant statement about the tem-

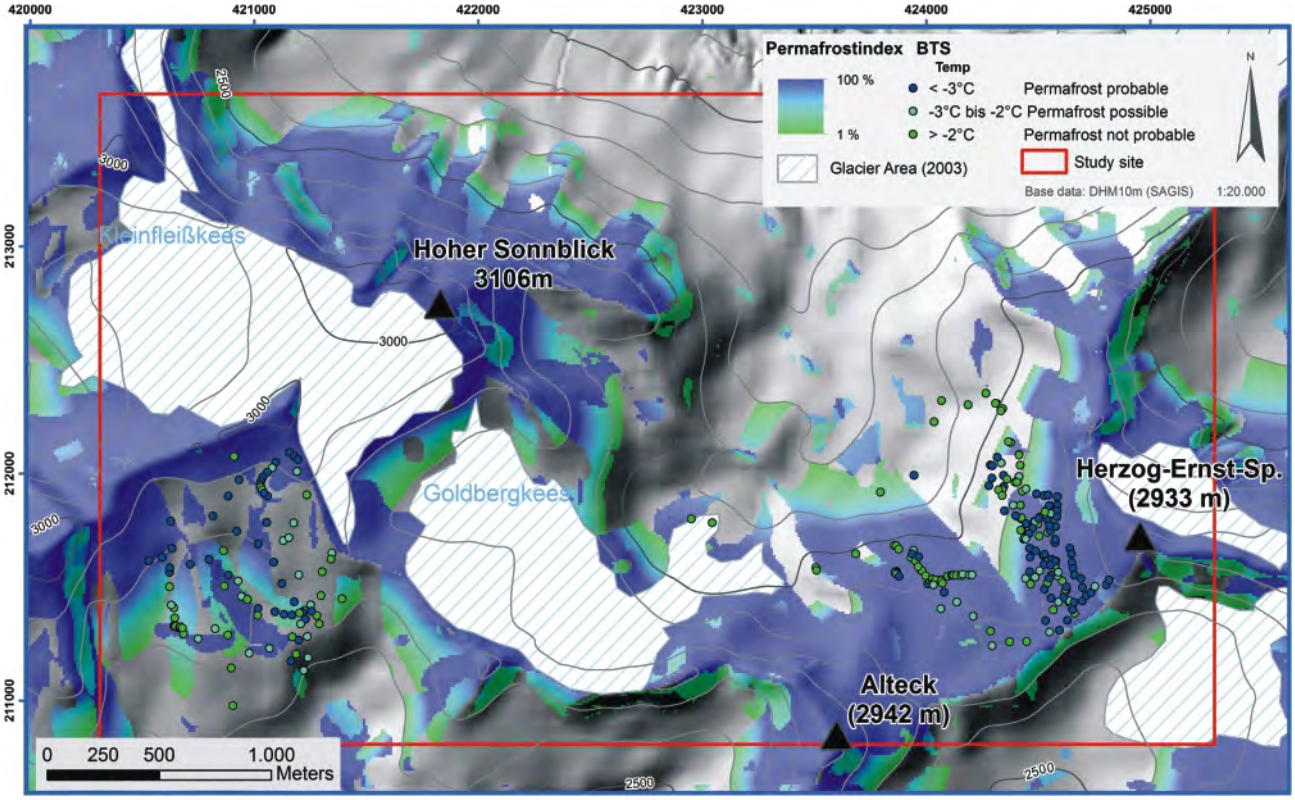

Figure 15: Map of permafrost distribution in the larger region of Hoher Sonnblick. The figure displays the measured BTS-values obtained within the PERSON-project. The red box indicates the zone used for quantification.

poral evolution of the ground temperatures and related permafrost. A long-time monitoring strategy is required for such conclusions, as well as for the spatial boundary of the permafrost body. Validation of an empirical permafrost distribution model for the study region against observed GST and BST measurements in the region of Hoher Sonnblick shows agreement for 60% of the sensor locations.

Acknowledgements

The seismic tomography was funded by the Österreichische Akademie der Wissenschaften (Austrian Academy of Science), ISDR project 'Permafrost in Austria'. The authors wish to express their special thanks to H.P. Hausmann, K. Lederer, and O. Simeoni for field assistance.

The GPR and 3D laser scanning survey was funded by the Central Institute for Meteorology and Geodynamics (ZAMG) as an internal research project in cooperation with the Ludwig Boltzmann Institute for Archaeological Prospection and Virtual Archaeology, special thanks to W. Neubauer, M. Kucera, E. Nau, T. Zitz for the field and data processing assistance.

Substantial financial support for this study came from the project “Permafrost in Austria – Part II: Permafrost in bedrock and its effect on ground stability and rock fall” funded by the Austrian Academy of Science (ÖAW), “PermaNET – Permafrost long-term monitoring network” funded within the Alpine Space Program of the European Union and PERSON – Permafrostmonitoring Sonnblick which have been funded by the Austrian Federal Ministry of Agriculture, Forestry, Environment and Water Management (BMLFUW).

The 10 x 10 m digital elevation model was provided by the province of Salzburg (SAGIS).

The comments of an anonymous reviewer and of Karl Krainer, which significantly improved the quality of the paper, are gratefully acknowledged.

References

Auer, I., Böhm, R., Leymüller, M. and Schöner, W., 2002. Das Klima des Sonnblicks – the climate of Sonnblick. Österreichische Beiträge zur Meteorologie und Geophysik, Heft 29.

Bertoldi, G., Rigon, R. and Over, T.M., 2006. Impact of watershed geomorphic characteristics on the energy and water budgets. Journal of Hydrometeorology 7(3), 389–403.

Dall'Amico, M., Endrizzi, S., Gruber, S. and Rigon, R. 2010. An energy-conserving model of freezing variably-saturated soil. The Cryosphere Discussion., 4, 1243–1276.

Draebing, D., and Krautblatter, M., 2011. Raw data analysis and sensitivity to initial model velocities of 2.5D-seismic refraction tomographies of permafrost in steep bedrock. Geophysical Research Abstracts 13, EGU2011-12785.

Endrizzi, S., 2009. Snow Cover Modelling at a Local and Distributed Scale over Complex Terrain. Monographs of the Doctoral School in Environmental Engineering 15, Department of Civil and Environmental Engineering, Universita degli Studi di Trento, Trento, Italy.

Gruber, S., 2005. Mountain permafrost: transient spatial modelling, model verification and the use of remote sensing, PhD dissertation, Department of Geography, University of Zurich, Switzerland, 123pp.

Haeberli, W., 1973. Die Basis-Temperatur der winterlichen Schneedecke als möglicher Indikator für die Verbreitung von Permafrost in den Alpen. Zeitschrift für Gletscherkunde und Glazialgeologie, 9, 221-227.

Haeberli, W., 1975. Untersuchungen zur Verbreitung von Permafrost zwischen Flüelapass und Piz Grialetsch (Graubünden). Mitteilungen der Versuchsanstalt für Wasserbau, Hydrologie und Glaziologie der ETH Zürich, Zürich, 221pp.

Haeberli, W., Rellstab, W. and Harrison, W. D., 1984. Geothermal effects of 18 ka BP ice conditions in the Swiss Plateau. Annals of Glaciology, 5, 56–60.

Haeberli, W., Guooong, C., Gorbunov, A. P. and Harris, S. A., 1993. Mountain permafrost and climatic change. Permafrost and Periglacial Processes. 4: 165-174.

Haeberli, W. and Hohmann, R., 2008. Climate, glaciers and permafrost in the Swiss Alps 2050: scenarios, consequences and recommendations. In Kane, D.I., Hinkel, K.M. (Eds.), Proceedings Ninth International Conference on Permafrost, Vol. 1, Institute of Northern Engineering, University of Alaska Fairbanks, pp. 607-612.

Hauck, C. and Vonder Mühll, D., 2003. Evaluation of geophysical techniques for application in mountain permafrost studies. Zeitschrift für Geomorphologie, Suppl.-Bd. 132, 161-190.

Hauck, C., Vonder Mühll D., and Maurer, H., 2003. DC resistivity tomography to detect and characterize mountain permafrost. Geophysical Prospecting, 51, 273-284.

Hauck, C., and Kneisel, C., 2008. Applied Geophysics in Periglacial Environments. Cambridge University Press, 256pp.

Hausmann, H., Krainer, K., Brückl, E. and Mostler, W., 2007. Internal structure and ice content of Reichenkar Rock Glacier (Stubai Alps, Austria) assessed by geophysical investigations. Permafrost and Periglacial Processes, 18, 351-367. DOI: 10.1002/ppp.60.

Hausmann, H., Staudinger, M., Brückl, E. and Riedl, C., 2010. Permafrost im Fels – Erste Ergebnisse der seismischen Tomographie am Sonnblickgipfel (3106 m, Hohe Tauern). Geo.Alp 7, p. 95.

Hilbich, C., Hauck, C., Scherler, M., Schudel, L., Völksch, I., Hoelzle, M., Vonder Mühll, D., and Mäusbacher, R., 2008. Monitoring mountain permafrost evolution using electrical resistivity tomography: A seven-year study of seasonal, annual and long-term variations at Schilthorn, Swiss Alps. Journal of Geophysical Research, 113, F01S90. doi:10.1029/2007JF00079.

Hilbich, C., 2010. Time-lapse refraction seismic tomography for the detection of ground ice degradation. The Cryosphere, 4, 243-259.

Hole, JA., 1992. Nonlinear high-resolution three-dimensional seismic travel time tomography. Journal of Geophysical Research, 97, 6553-6562.

Hölzle, M., 1994. Permafrost und Gletscher im Oberengadin: Grundlagen und Anwendungsbeispiele für automatisierte Schätzverfahren. VAW Mitteilungen 132, Zürich.

Keller, F., 1992. Automated mapping of mountain permafrost using the program PERMAKART within the geographical information system ARC/INFO. Permafrost and Periglacial Processes 3, 2, 133-138.

Kneisel, C., Hauck, C., Fortier, R., and Moorman, B.J., 2008. Advances in geophysical methods for permafrost investigations. Permafrost and Periglacial Processes, 19: 157-178. DOI: 10.1002/ppp.61.

Kohnen, H., 1974. The temperature dependence of seismic waves in ice. Journal of Glaciology, 13, 144–147.

Krainer, K. and Mostler, W., 2000. Reichenkar rock glacier: a glacier derived debris-ice system in the Western Stubai Alps, Austria. Permafrost and Periglacial Processes, 11, 267-275.

Krautblatter, M. and Hauck, C., 2007. Electrical resistivity tomography monitoring of permafrost in solid rock walls. Journal of Geophysical Research, Earth-Surface, 112, doi:10.1029/2006JF000546.

Krautblatter, M., Verleysdonk, S., Fores-Orozco, A. and Kemna, A., 2010. Temperature-calibrated imaging of seasonal changes in permafrost rock walls by quantitative electrical resistivity tomography (Zugspitze, German/Austrian Alps). Journal of Geophysical Research, Earth Surface, 115, F02003.

Lieb, G.K., 1991. Die horizontale und vertikale Verteilung der Blockgletscher in den Hohen Tauern (Österreich). Zeitschrift für Geomorphologie N.F., 35, 345-365.

Lieb, G.K., 1998. High-Mountain permafrost in the Austrian Alps (Europe). Proceedings of the 7th International Conference on Permafrost, Yellowknife, Canada, 23-27 June, 1998, pp-663-668.

Neubauer, W., Eder-Hinterleitner, A., Seren, S. and Melichar, P., 2002. Georadar in the Roman Civil Town Carnuntum, Austria: An Approach for Archaeological Interpretation of GPR Data. Archaeological Prospection, 9, 135–156. DOI: 10.1002/arp.183.

Noetzli, J., 2008. Modeling transient three-dimensional temperature fields in mountain permafrost. PhD Thesis, Department of Geography, University of Zurich, Zurich, 142 pp.

Noetzli, J. and Gruber, S. 2009. Transient thermal effects in Alpine permafrost. The Cryosphere, 3, 85–99.

Piemonte, A., 2011. WP4-Final Report - Handbook to establish alpine permafrost monitoring network. <http://www.permanet-alpinespace.eu/archive/pdf/WP4_handbook.pdf> last Access: 30.01.2012.

Pogliotti, P, Cremonese, E, Morra di Cella, U, Gruber, S. and Giardino, M., 2008. Thermal diffusivity variability in alpine permafrost rock walls. In: 9th International Conference on Permafrost, Fairbanks, Alaska, 29 June 2008 - 03 July 2008, 1427-1432.

Pomeroy, J.W., Gray, D.M., Landine, P.G., 1993. The Prairie Blowing Snow Model: characteristics, validation, operation. Journal of Hydrology, 144, 165-192.

Rigon, R., Bertoldi, G. and Over, T.M., 2006. GEOtop: a distributed hydrological model with coupled water and energy budgets. Journal of Hydrometeorology, 7, 371–388.

Schober, C, 2002. Zur Geologie des Sonnblicks unter Einbeziehung der Erosionsgefährdung und angepasster Sanierungsmaßnahmen. Jahresberichte des Sonnblickvereins 98-98: 3-24.

Schöner, W., Böhm, R. and Auer, I., 2012. 125 years of high-mountain research at Sonnblick Observatory (Austrian Alps) from “the house above the clouds” to a unique research platform. Theoretical and Applied Climatology, DOI 10.1007/s00704-012-0689-8.

Scott, W.J., Sellmann, P. and Hunter, J.A., 1990. Geophysics in the study of permafrost. In Geotechnical and Environmental Geophysics, Vol. 1: Review and Tutorial, Society of Exploration Geophysicists Investigation in Geophysics no. 5, 355–38.

Vonder Mühll, D., 1996. Drilling in alpine permafrost. Norwegian Journal of Geography (Norsk Geografisk Tidsskrift), 50 (1), 17-24. DOI: 10.1080/0029195960855234.

Vonder Mühll, D., Hauck, C. and Gubler, H., 2002. Mapping of mountain permafrost using geophysical methods. Progress in Physical Geography, 26(4), 643-660.

Vonder Muehll, D., Noetzli, J. and Roer, I., 2008. PERMOS – a comprehensive monitoring network of mountain permafrost in the Swiss Alps. Proceedings of the 9th International Conference on Permafrost, Fairbanks, US, 1869-1874.

Wegmann, M., Gudmundsson, G.H. and Haeberli W., 1998. Permafrost changes in rock walls and the retreat of Alpine glaciers: a thermal modelling approach. Permafrost and Periglacial Processes, 9, 23-33.

Received: 7 March 2012
Accepted: 20 November 2012

Wolfgang SCHÖNER[1)*)], Lorenz BOECKLI[5)], Helmut HAUSMANN[1)4)], Jan-Christoph OTTO[3)], Stefan REISENHOFER[1)], Claudia RIEDL[2)] & Sirri SEREN[1)]

[1)] Central Institute for Meteorology and Geodynamics (ZAMG), Vienna, Austria;

[2)] Central Institute for Meteorology and Geodynamics (ZAMG), Salzburg, Austria;

[3)] University Salzburg, Institute of Geology and Geography, Salzburg, Austria;

[4)] Institute of Geodesy and Geophysics, Vienna University of Technology, Vienna, Austria;

[5)] University of Zürich, Institute of Geography, Zürich, Switzerland;

[*)] Corresponding author, wolfgang.schoener@zamg.ac.at